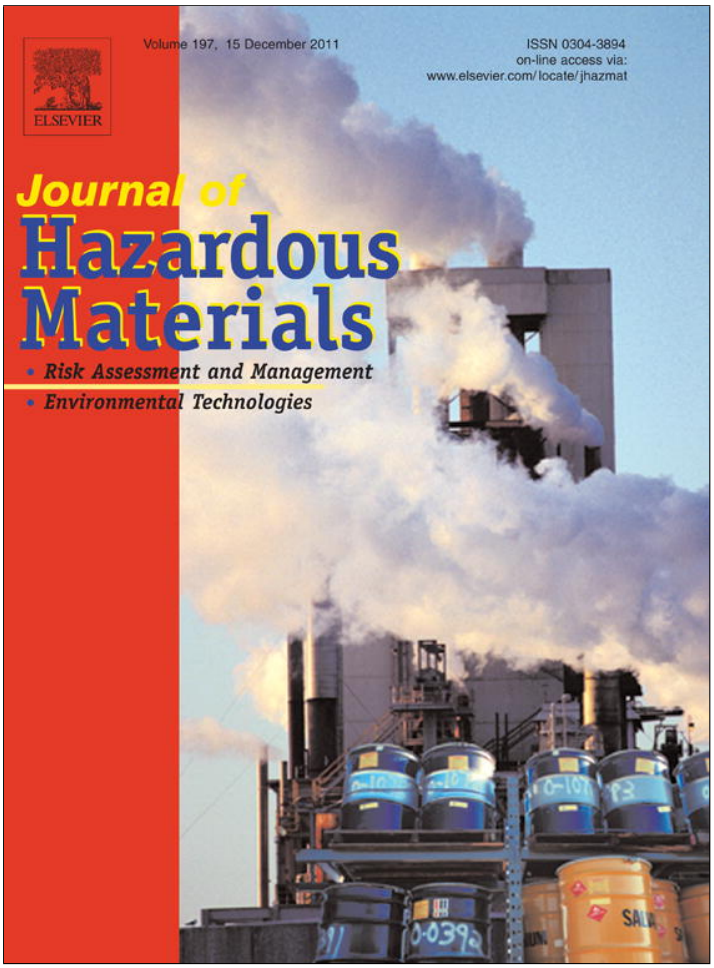

Journal of Hazardous Materials 197 (2011) 229–236

Contents lists available at SciVerse ScienceDirect

Journal of Hazardous Materials

journal homepage: www.elsevier.com/locate/jhazmat

Photocatalytic degradation kinetics and mechanism of antivirus drug-lamivudine in TiO_2 dispersion

Taicheng An[a,*], Jibin An[a,b,d], Hai Yang[a,d], Guiying Li[a], Huixia Feng[b], Xiangping Nie[c]

[a] State Key Laboratory of Organic Geochemistry and Guangdong Key Laboratory of Environmental Resources Utilization and Protection, Guangzhou Institute of Geochemistry, Chinese Academy of Sciences, Guangzhou 510640, China
[b] College of Petrochemical Technology, Lanzhou University of Technology, Lanzhou 730050, China
[c] Institute of Hydrobiology, Jinan University, Guangzhou 510632, China
[d] Graduate School of Chinese Academy of Sciences, Beijing 100049, China

ARTICLE INFO

Article history:
Received 23 June 2011
Received in revised form
20 September 2011
Accepted 21 September 2011
Available online 28 September 2011

Keywords:
Photocatalytic degradation
Lamivudine
Kinetics
Central composite design
Mechanism

ABSTRACT

Photocatalytic degradation kinetics of antivirus drug-lamivudine in aqueous TiO_2 dispersions was systematically optimized by both single-variable-at-a-time and central composite design based on the response surface methodology. Three variables, TiO_2 content, initial pH and lamivudine concentration, were selected to determine the dependence of degradation efficiencies of lamivudine on independent variables. Response surface methodology modeling results indicated that degradation efficiencies of lamivudine were highly affected by TiO_2 content and initial lamivudine concentration. The highest degradation efficiency was achieved at suitable amount of TiO_2 and with maintaining initial lamivudine concentration to a minimum. In addition, the contribution experiments of various primary reactive species produced during the photocatalysis were investigated with the addition of different scavengers and found that hydroxyl radicals was the major reactive species involved in lamivudine degradation in aqueous TiO_2. Six degradation intermediates were identified using HPLC/MS/MS, and photocatalytic degradation mechanism of lamivudine was proposed by utilizing collective information from both experimental results of HPLC/MS/MS, ion chromatography as well as total organic carbon and theoretical data of frontier electron densities and point charges.

1. Introduction

The presence of pharmaceutical ingredients in aqueous environment has raised increasing concerns in recent years. Typical sources of them are sewage effluents, hospital waste, animal excrements, and improper disposal of unused drugs. However, conventional sewage treatment plants are not able to effectively eliminate these pharmaceutical residues and as a result they are continuously discharged into environmental waters. Numerous studies have documented that the pharmaceutical residues are persistent in water owning to its continuous discharge into aqueous environment, which has ubiquitously been detected in groundwater and effluent water [1–5]. These pharmaceutical residues include antibiotics, anticonvulsants, analgesics, lipidregulators, β-blocks, antihistamines and contraceptive drugs ranging from ng L^{-1} to μg L^{-1} level [1,2]. Although these levels are much low compared with other conventional organic pollutants, a wide range of investigations reported that these drugs have raised concerns due to their potential impact on environment and human, such as the aquatic toxicity, the genotoxicity, and endocrine disruption as well as the developing of bacteria resistance to antibiotics [3–5].

Lamivudine, an antivirus drug, belonging to the class of nucleoside analog reverse transcriptase inhibitor, has received recent attention because of its wide use for potent inhibition effect on HIV and HBV. However, only one work reported its concentration in water and as obtained lower than ng L^{-1} detected by HPLC/MS/MS [6]. Little is known concerning its environmental behavior and the fate in water environments, except that lamivudine is very stable to various forced decomposition conditions of hydrolysis (neutral), UV light and thermal stress as well as low concentration of H_2O_2 [7]. Thus, lamivudine may not easily be metabolized and can be excreted into the sewage by the human or animal metabolism. Hence, it is very urgent to understand the fates, risk as well as the degradation patterns in the water environments.

Advanced oxidation processes (AOPs), with highly reactive hydroxyl radicals (•OH radicals) as the main oxidative species, can degrade water soluble environmental pharmaceuticals effectively [8,9]. Among various AOPs, TiO_2 heterogeneous photocatalysis has been proven to be a promising technology for the decontamination of these compounds [9,10]. However, to our knowledge,

* Corresponding author. Tel.: +86 20 85291501; fax: +86 20 85290706.
E-mail address: antc99@gig.ac.cn (T. An).

0304-3894/$ – see front matter © 2011 Elsevier B.V. All rights reserved.
doi:10.1016/j.jhazmat.2011.09.077

photocatalytic degradation of antivirus pharmaceuticals has never been attempted yet. Furthermore, in most conventional studies, photocatalytic kinetics optimization is usually carried out by the single-variable-at-a-time (SVAT, the most common practice holding all other variables constant) method [11,12]. Nevertheless, SVAT approach possessed lots of drawbacks, such as time-consuming and the absence of interactions between different variables as well as the inefficiency to predict the true optimum. An alternative method, central composite design (CCD) based on response surface methodology (RSM) can overcome all these shortcomings mentioned above [11,13]. It is because the RSM can explore the relationships between several variables and one or more response variables. The main idea of RSM is to use a sequence of designed experiments to obtain an optimal response.

Thus, in this paper, photocatalytic degradation kinetics of an antivirus drug, lamivudine, was studied in aqueous TiO_2 suspension under UV light irradiation. Various affecting parameters such as TiO_2 content, pH and initial lamivudine concentration, were optimized by the SVAT method without considering the interaction of different variables. Simultaneously, CCD based on RSM was employed to assess the individual and interaction effects of several variables on photocatalytic degradation efficiencies of lamivudine, and to propose more accurate model for the photocatalytic kinetics. Furthermore, the contributions of various reactive species to the degradation rate of lamivudine were indirectly examined in detail with addition of different scavengers. In addition, photocatalytic degradation mechanism of lamivudine was proposed tentatively based on the experimental results of HPLC/MS–MS as well as the theoretically calculated data of the frontier electron densities (FEDs) and the point charges.

2. Materials and methods

2.1. Materials

Lamivudine (≥99% purity) was purchased from Tokyo Chemical Industry Co., Ltd. (TCI) and used without any purification. Titanium dioxide (P25 TiO_2, Degussa, Germany) was used as the photocatalyst without pretreatment. HPLC grade water was obtained by Millipore Milli-Q system, which was treated by constant illumination with a xenon arc lamp at 172 nm to keep total organic carbon concentration of water below 13 $\mu g\,L^{-1}$. Methanol (HPLC grade) was obtained from Sigma. Other reagents were all analytical grade.

2.2. Photocatalytic procedure

The experiments were carried out in a 150-mL open Pyrex reactor with a double-walled cooling-water jacket to keep the constant room temperature of the solution throughout the experiment. The light source was a high-pressure mercury lamp (GGZ-125, Shanghai Yaming Lighting, E_{max} = 365 nm) and located in parallel with the photocatalytic reactor to provide the irradiation (the experiment apparatus see Fig. S1). The light intensity at the surface of Pyrex tube was maintained at 0.38 mW/cm^2. Certain amount of TiO_2 was added into a 150 mL solution (100 μM lamivudine) to conduct the degradation experiments according to the experimental designed values. Prior to illumination, the suspension was stirred in the dark for 30 min to achieve the adsorption–desorption equilibrium. Once the lamivudine concentration was stabilized, the solution was immediately irradiated with UV light, signaling the start of the photocatalytic degradation. At given time intervals, a portion of sample was collected and filtered through 0.22 μm Millipore filters to remove TiO_2 particles for further analysis.

2.3. Design of experiment

The chemometric approach was applied using a CCD with the form of RSM. Analysis of the experimental data was supported by the Design-Expert software (trail version 8, Stat-Ease, Inc., MN, USA).

2.4. Analytical procedures

The concentration of lamivudine was analyzed at 30 °C using Shimadzu LC20AB series HPLC system with a Kromasil C18 column (250 mm × 4.6 mm i.d.). The mobile phase was a mixture of 80% (v/v) water (pH value set at 3.0 with phosphoric acid) and 20% methanol with a flow rate of 1 $mL\,min^{-1}$. The detection wavelength was 275 nm and the injection volume was 20 μL.

Lamivudine and its degradation intermediates were measured using HPLC/MS/MS. The system was an Agilent 1200 series HPLC with a Kromasil C18 column, SIL-HT autosampler, G1311A quaternary pump and API 3000 mass analyzer. HPLC separations were performed at 0.5 $mL\,min^{-1}$ with mobile phase of 25% CH_3OH and 75% formic acid solution (5 mM). An electrospray interface (ESI) was used for the MS and MS/MS measurements in positive ionization mode and full scan acquisition between m/z of 50 and 500. The collision energy varied according to the requirement of the different measurements, and the other parameters were set as follows: the source block and desolvation temperatures were 130 and 400 °C, respectively. The desolvation and nebulizer gas (N_2) flow rate was set as 6 $L\,min^{-1}$ and argon was used as a collision gas at 250 kPa.

A Dionex ion chromatograph equipped with a conductimeter detector was used for the determination of ammonium ions with a column CS12A and 25 mM H_2SO_4 as eluent, at a flow rate of 1 $mL\,min^{-1}$. In such conditions, the retention time of ammonium ion is 5.03 min. The anions were also analyzed by using AS9HC anionic column and a mixture solution of $NaHCO_3$ (4.5 mM) and K_2CO_3 (0.8 mM) as eluent, at flow rate of 1 $mL\,min^{-1}$. The retention times were 14.04 and 22.18 min for nitrate and sulphate ions, respectively.

To determine the extent of mineralization, total organic carbon (TOC) contents of samples were measured with a Shimadzu TOC-5000 analyzer (catalytic oxidation on Pt at 680 °C). Triplicate analyses were performed for each sample.

2.5. Frontier electron densities and point charges calculations

Molecular orbital calculations were carried out using Gaussian 03 program (Gaussian, Inc.) at the single determinant (HF/3-21) level with the optimal conformation having a minimum energy obtained at the B3LYP/6-31G* level. According to Frontier Orbital Theory, the electrophilic reaction most likely occurred in atoms with high value of the highest occupied molecular orbital (HOMO), and nucleophilic reaction most likely occurred in atoms with high value of the lowest unoccupied molecular orbital (LUMO). Thus the HOMO and LUMO FEDs of lamivudine molecule were calculated, respectively. The values of $(FED^2_{HOMO} + FED^2_{LUMO})$ and $2FED^2_{HOMO}$ were obtained to predict the initial attack sites for •OH radicals addition and photoholes (electron extraction) to (from) lamivudine molecule, respectively [14,15]. The point charges were also calculated with the help of natural bond orbital (NBO) to predict the chemisorption position of lamivudine onto the TiO_2 [16]. All the calculations were performed on a personal computer.

3. Results and discussion

3.1. Single-variable kinetics optimization

Photocatalytic degradation of lamivudine was carried out varying TiO_2 concentration from 0.25 to 3.00 $g\,L^{-1}$, whereas the other

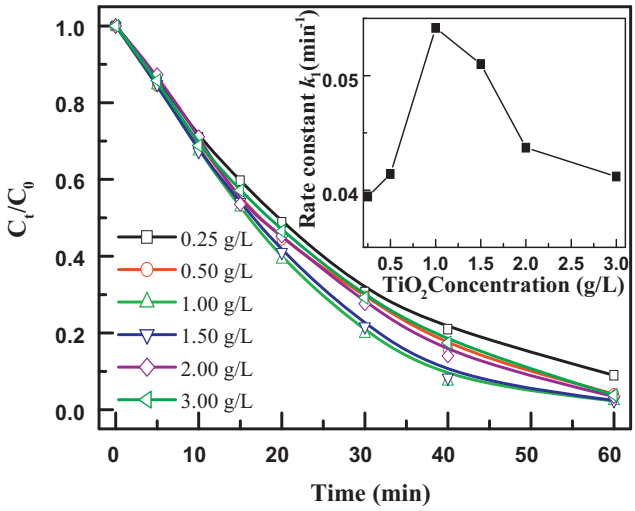

Fig. 1. Influence of TiO_2 concentration on the rate constants of the photocatalytic degradation of lamivudine: [Lamivudine] = 100 μM and pH value 7.0.

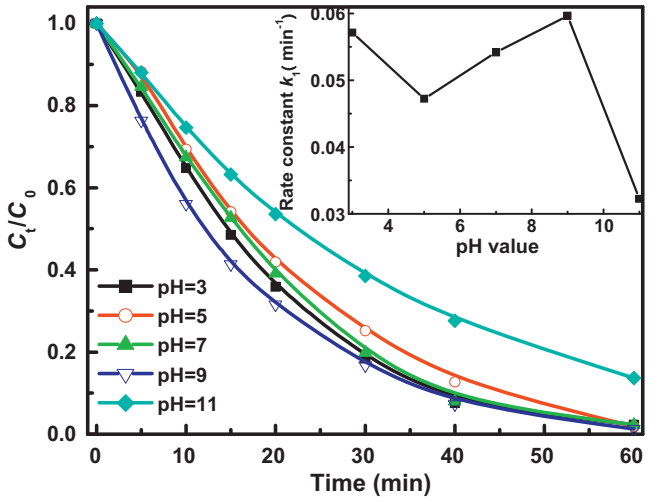

Fig. 2. Influence of pH value on the rate constants of the photocatalytic degradation of lamivudine: [Lamivudine] = 100 μM, and [TiO_2] = 1.00 g L^{-1}.

parameters remained constant with lamivudine concentration of 100 μM and at pH 7.0. The dependence of TiO_2 concentrations on the degradation efficiencies was shown in Fig. 1. With the increase of the degradation time, the degradation efficiencies initially increased swiftly with the increase of TiO_2 concentrations and peaked at 1.00 g L^{-1}, then decreased gradually.

A number of studies have documented that photocatalytic degradation kinetics of various pharmaceuticals over illuminated TiO_2 can be fitted the Langmuir–Hinshelwood kinetics model [10,17–19]. When the concentration of pharmaceuticals is in the scale of millimoles, KC can be neglected with respect to 1 ($KC \ll 1$), and an apparent first-order model can be assumed as Eq. (1):

$$-r = \frac{dc}{dt} = kKC = k_{app}C \quad (1)$$

and hence the Eq. (1) gives Eq. (2):

$$\ln\left(\frac{C_0}{C}\right) = k_{app}t + \text{constant} \quad (2)$$

where k_{app}, the apparent first-order rate constant, can be obtained from the slope upon the linear regression verse the degradation time.

Accordingly, the relationship between the apparent rate constant and TiO_2 concentrations was also investigated and shown in the inset of Fig. 1. It can be easily found that with the increase of TiO_2 concentrations, the apparent rate constant firstly increased from 0.0395 min^{-1} at 0.25 g L^{-1} to 0.0542 min^{-1} at 1.00 g L^{-1}, and then decreased to 0.0412 min^{-1} at 3.00 g L^{-1}. It is because that the more TiO_2 particles were excited by UV light, the more reactive species were produced, thus the higher rate constants were obtained with the increase of TiO_2 concentration. However, with further increase of TiO_2 concentrations from 1.00 g L^{-1} to 3.00 g L^{-1}, the light penetration will decrease rapidly, and the TiO_2 particles were subsequently less excited and deactivated probably *via* TiO_2 particle–particle collision.

Effect of pH on the photocatalytic degradation of lamivudine was also investigated by adjusting pH values from 3.0 to 11.0 at 100 μM lamivudine and 1.00 g L^{-1} TiO_2. Fig. 2 shows that the degradation efficiencies gradually increased with the increase of reaction time at all tested pH value. After 60 min, the degradation efficiencies were around 98% and not affected so widely by pH value ranged from 3.0 to 9.0, while the degradation efficiency dropped to 86.3% with the further increase of pH to 11.0. In addition, the relationship between the apparent rate constant and pH value was also studied (inset of Fig. 2). The apparent rate constants first decreased from 0.0571 min^{-1} at pH 3.0 to 0.0472 min^{-1} at pH 5.0, but increased to 0.0597 min^{-1} at pH 9.0, and then decreased again to 0.0322 min^{-1} at pH 11.0.

It is well known that either the adsorption process or the surface reaction is the rate-determining step for catalytic reaction. Thus, the photocatalytic degradation was strongly depended on the adsorption/desorption characteristics [17,20,21]. That is, photocatalytic degradation occurred mainly on the surface of TiO_2 by oxidation reactions with photoholes or •OH radicals [17]. Thus, in this paper, the dependence of the degradation rate constant on pH value was explained as follows: firstly, TiO_2 particles has an isoelectric point approximately 6.3, indicating that the surface of TiO_2 particles has positive charge at pH < 6.3 and negative charge at pH > 6.3 [22]. Secondly, the pk_a value of lamivudine was 4.4 [6]. When pH value is less than 4.4, lamivudine mainly exists as positive molecules, while it exists as neutral forms when pH value is higher than 4.4. That is, at low pH value, for example at 3.0, low adsorption will obtain due to the repelling effect of two positive charges. With increasing pH value, the surface positive charge of TiO_2 gradually decreases, and the neutral form of lamivudine was also increased. Hence, the adsorption amounts of neutral lamivudine onto positive TiO_2 particles increased slowly. After pH value >6.3, the surface of TiO_2 particles become negative charge, while lamivudine still keep as a neutral form. Thus we can predict that the adsorption of lamivudine onto TiO_2 is much larger at basic solution than that at acid solution. In order to confirm this hypothesis drawn from the above results, the adsorption kinetics of lamivudine onto TiO_2 were also carried out, and the results were shown in Fig. S2. From the figure, however, it can be found that regardless any pH value, the adsorption efficiencies varied very slightly, and almost all the adsorption efficiencies are very small and neglectable (less than 1% except pH value 7.0 with 2%) within 60 min adsorption. Thus it can be concluded that the adsorption between lamivudine and TiO_2 particles was very weak and subsequent influence on the degradation rate of lamivudine was slight. The surface reaction hypothesis may not be suitable for this study and the photocatalytic degradation of lamivudine did not controlled by the surface reaction.

The dependence of the degradation efficiencies on initial lamivudine concentration was also carried out (Fig. S3). From the figure, within 60 min illumination, lamivudine can be completely degraded with an initial concentration of 50 μM, while only less than 70% of lamivudine was decomposed with an

Table 1
Scavengers used, reactive species quenched, and rate constants with quenched RSs.

	Scavengers	RSs quenched	k (min^{-1})	R^2
Lamivudine	N_2 and $K_2Cr_2O_7$	$H_2O_2/O_2^{\bullet-}$	0.0338	0.99
	KI	$h_{vb}^+/^{\bullet}OH$	0.0004	0.87
	Isopropanl	$^{\bullet}OH$	0.0027	0.94
	NO	/	0.0542	0.98

initial concentration of 200 μM. With increasing initial concentration from 50 to 200 μM, the degradation efficiencies decrease significantly. The dependence of the degradation rate on initial lamivudine concentration was also studied and shown in inset of Fig. S3. Seen from the figure, the apparent rate constant decreased rapidly from 0.1073 min^{-1} at 50 μM to 0.0788 min^{-1} at 100 μM, and then finally to 0.02203 min^{-1} at 200 μM initial concentration. It is because that more pharmaceuticals existed in solution can absorb more photons, thus less TiO_2 particles can be activated due to the decrease of the photos absorption to the surface of TiO_2, which may restraint the generation of the oxidants.

3.2. Contribution of different reactive species

According to the photocatalytic mechanism, the photogenerated electrons can be scavenge by oxygen to form $O_2^{\bullet-}/HO_2^{\bullet}$ radical and H_2O_2. On the other hand, the photogenerated holes also can be partially captured by OH^- or H_2O to form $^{\bullet}OH$ radicals [23]. Thus various primary reactive species, such as h_{vb}^+, $^{\bullet}OH$, $O_2^{\bullet-}/HO_2^{\bullet}$ as well as H_2O_2, can be produced during the photocatalytic degradation of organics [23,24]. To distinguish the contribution of these reactive species to the photocatalytic degradation of lamivudine, different scavengers were employed to investigate their indirect effects. Isopropanol was added into the solutions to scavenge $^{\bullet}OH$ radicals in bulk solution [25,26], potassium iodine (KI) was selected as scavenger of both $^{\bullet}OH$ radicals and photoholes [27], and Cr(VI) was used as an electron scavenger with both exclusion O_2 from solution by purging nitrogen [24]. The scavengers used for different reactive species and the corresponding apparent first-order rate constants with or without scavengers were summarized in Table 1.

As shown in Fig. 3, a complete degradation of lamivudine can be achieved within 60 min without addition of any scavengers, which can be attributed to the combined effects of all reactive species. However, the formed H_2O_2 and $O_2^{\bullet-}/HO_2^{\bullet}$ can be excluded in the presence of 0.1 M $K_2Cr_2O_7$ upon purging with nitrogen, the photocatalytic degradation of lamivudine was partially

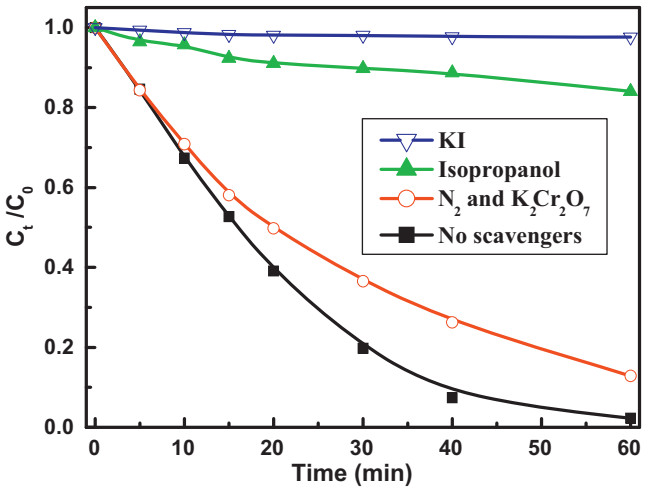

Fig. 3. The photocatalytic degradation of lamivudine without or with scavengers: [Lamivudine] = 100 μM, [TiO_2] = 1.00 g L^{-1}, and pH value 7.0.

hindered for 37.6% with the decrease of the rate constants from 0.0542 to 0.0338 min^{-1}. This indicated that the contribution of e_{cb}^- is very limited when oxygen is supplied in the solution. In fact, the reactive species such as $O_2^{\bullet-}/HO_2^{\bullet}$ and H_2O_2 produced from e_{cb}^- reduction can be finally transformed into the $^{\bullet}OH$ radicals under UV irradiation and then involved into the oxidation of lamivudine [24]. Similarly, when both h_{vb}^+ and $^{\bullet}OH$ radical were suppressed by I^-, the rate constant decreased for more than 99.3% from 0.0542 to 0.0004 min^{-1}. This demonstrates that both h_{vb}^+ and $^{\bullet}OH$ radical together are responsible for nearly 99.3% of the rate of the photocatalytic degradation of lamivudine. Furthermore, in order to distinguish the contribution of $^{\bullet}OH$ radical from photohole, 0.1 M isopropanol was added into the solutions to scavenge $^{\bullet}OH$ radical only. Results indicated that the rate constant was also significantly decreased for more than 95.0% from 0.0542 to 0.0027 min^{-1}. Thus, it can be concluded that h_{vb}^+ alone only contributes 4.3% to the degradation rate of lamivudine in this system. The obtained low contributions of photoholes also can further confirm our above-drawn conclusion that the photocatalytic degradation of lamivudine do not controlled by the surface reaction in this case.

3.3. Multivariable experimental design

Obviously, from above single-variable optimization experiments, photocatalytic degradation efficiencies of lamivudine can be affected by TiO_2 concentration, pH value and initial lamivudine concentration. However, it just optimized the degradation kinetics by varying one variable at a time while fixing all other variables at a specific set of conditions. It is difficult to find interaction effects of these single variables on the photocatalytic degradation of lamivudine. Thus, multivariable experimental design was performed according to CCD based on RSM [28–30]. For comparison, three experimental variables, TiO_2 concentration, initial pH value and initial concentration of lamivudine, were also selected in the multivariable experimental design.

This rotatable experimental plan was carried out with CCD, which consisted of 17 experiments determined by expression: $N = 2^n + 2n + C_0$, where N is total number of experiments required, n is the number of variables, $2n$ is axial runs and C_0 is center point runs. All these experiments counted from three blocks: (a) three variables ($n = 3$) at two levels: low (−1) and high (+1), full factorial design $2^3 = 8$; (b) 6 ($2n$) axial points located at the central and both extreme levels; (c) 3 central replicates of central points. Table S1 summarizes the levels for each variable involved in the design strategy, and all these levels were chosen based on our previous SVAT experiments. All experimental data in CCD for photocatalytic degradation of lamivudine were listed in Table 2. Experimental condition for response factor (Y) corresponded to photocatalytic degradation efficiencies of lamivudine (%) after 30 min irradiation.

The Design-Expert software was employed to find the best fitted model. A semi-empirical second-order polynomial equation consisting of 10 statistically significant coefficients was obtained from the data analysis for the degradation efficiencies of lamivudine (%) after 30 min irradiation. The response factor (Y) was calculated as a function of the independent variables as follows:

$$Y = 84.10 - 1.79x_1 - 0.048x_2 - 3.67x_3 + 0.0001x_1x_2 - 1.13x_1x_3 + 0.62x_2x_3 - 0.28x_1^2 - 0.86x_2^2 + 0.29x_3^2 \quad (4)$$

The coefficients in the polynomial equation represent the weight of each variable (x_1, x_2, and x_3) corresponding to TiO_2 concentration, initial pH value, and initial lamivudine concentration, respectively, as well as the interaction between them, including the cross-product coefficients and the quadratic coefficients. The experimental values (Y_{exp}) against the predicted responses (Y_{cal}) by

Table 2
Experimental data in central composite design for photocatalytic degradation of lamivudine.

Pattern	Block	Variables in uncodified levels			Y_{exp}	Y_{cal}
		x_1 (TiO_2 concentration)	x_2 (pH value)	x_3 (La. concentration)		
−1−1−1	1	1.0	5.5	60	88.6	88.3
+1−1−1		3.0	5.5	60	87.4	86.3
−1+1−1		1.0	9.5	60	88.7	86.9
+1+1−1		3.0	9.5	60	85.9	85.6
−1−1+1		1.0	5.5	90	82.9	81.9
+1−1+1		3.0	5.5	90	75.6	76.1
−1+1+1		1.0	9.5	90	83.9	83.1
+1+1+1		3.0	9.5	90	78.2	77.2
−α00	2	0.3	7.5	75	84.6	86.3
+α00		3.7	7.5	75	80.2	80.3
0−α0		2.0	4.1	75	81.6	81.7
0+α0		2.0	10.9	75	79.9	81.6
00−α		2.0	7.5	50	90.0	91.1
00+α		2.0	7.5	100	78.0	78.7
000	3	2.0	7.5	75	84.2	84.1
000		2.0	7.5	75	84.2	84.1
000		2.0	7.5	75	84.2	84.1

Y: the degradation efficiencies of lamivudine (%) after 30 min irradiation.

the model for the degradation efficiencies of lamivudine (%) with a good correlation (R^2 = 0.9473) indicate that this model explains the experimental range studied very well, as shown in Fig. S4.

Evaluated by *P* values (significant probability values), if the *P* value was smaller than 0.05, that means the model terms are very significant. In this case, seen from Table 3, the variables of TiO_2 concentration (x_1) and initial concentration of lamivudine (x_3) were highly significant because two *P* values were as low as 0.0023 and <0.0001, while the variable of pH value was much less significant (*P* values, 0.9034). That is, the response factors (*Y*) were significantly affected by two former variables, but much less affected by the later one. Similarly, the *P* values from interaction variable x_1x_3 obtained as 0.0596 indicated that this variable was significant than other cross variables. Thus, two-dimension contour and response surface plots were carried out in order to determine the dependence of the response factor (*Y*) on the cross variable x_1x_3, and the results were shown in Fig. 4a and b. It can be seen that the degradation efficiencies decrease with the increase of initial lamivudine concentration, and the highest degradation efficiencies occurred when TiO_2 dosage at suitable concentration and with keeping initial concentration of lamivudine to a minimum.

To confirm the validity and accuracy of the model, the experiments were carried out at the optimal conditions for the highest photocatalytic efficiency of lamivudine. The software optimized degradation efficiencies was 88.59% at the optimized conditions of TiO_2 concentration of 1.00 g L^{-1}, pH value of 6.7, and lamivudine concentration of 60 μM, respectively (Fig. S5). The experimental degradation efficiency of 87.1% was very close to the predicted value, indicating the adequacy of the obtained model to optimize photocatalytic degradation of lamivudine.

Table 3
Response surface model regression coefficient and *P*-value for response.

Term	Variable	Regression coefficient	*P*
TiO_2 concentration	x_1	−1.79	0.0023
pH value	x_2	−0.048	0.9034
Initial concentration of lamivudine	x_3	−3.67	<0.0001
TiO_2 conc. × pH value	x_1x_2	0.0001	1.0000
TiO_2 conc. × Lamivudine conc.	x_1x_3	−1.13	0.0596
pH value × Lamivudine conc.	x_2x_3	0.62	0.2523
TiO_2 conc. × TiO_2 conc.	x_1^2	−0.28	0.5351
pH value × pH value	x_2^2	−0.86	0.0814
Lamivudine conc. × Lamivudine conc.	x_3^2	0.29	0.5135

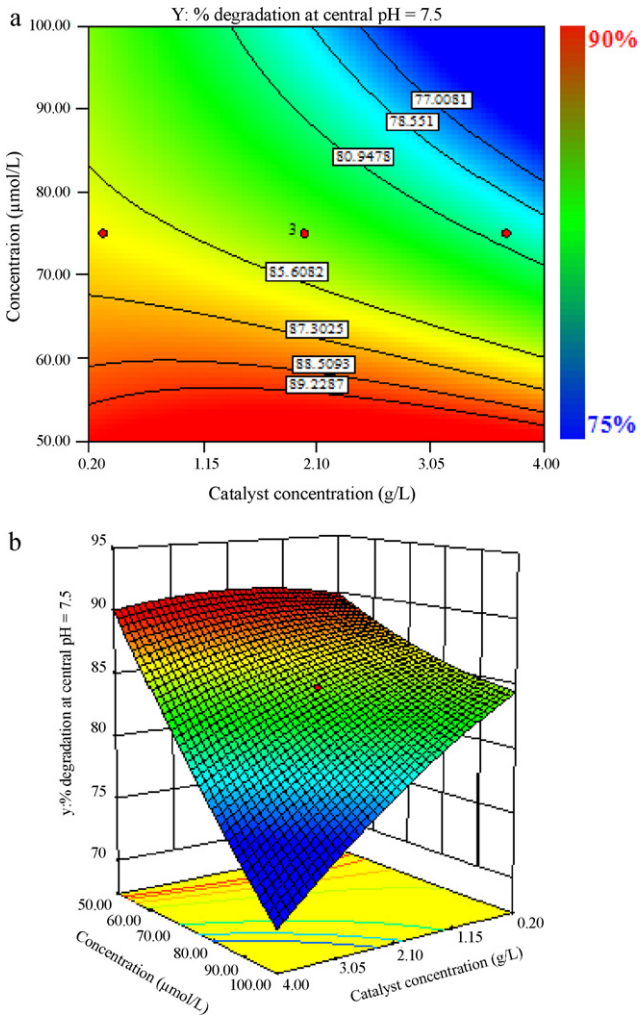

Fig. 4. Two-dimension contour and response surface plots for interaction between TiO_2 concentration (x_1) and initial lamivudine concentration (x_3) with pH value fixed to 7.5.

3.4. Preliminary reaction mechanism

The photocatalytic degradation mechanism of lamivudine was elucidated from HPLC/MS–MS results coupled with the calculated

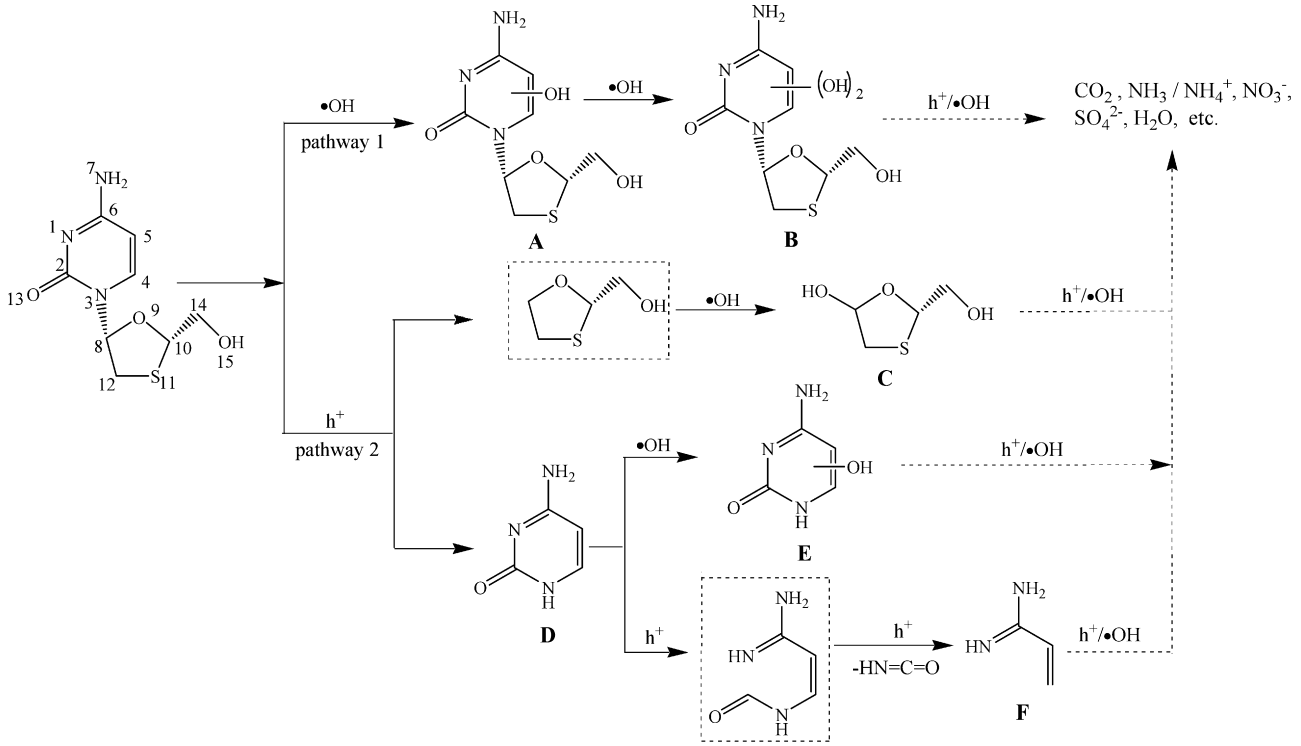

Scheme 1. Proposed photocatalytic degradation mechanism of lamivudine in TiO_2 suspension.

data of the FEDs and point charges. According to HPLC/MS/MS analyses, six intermediates were identified, and listed in Table S2. It can be found that the intermediates with m/z value of 246 corresponding to the addition of 16 mass units (monohydroxylated intermediates (A)) to lamivudine and 262 corresponding to the dihydroxylated derivatives (B), were all identified successively (Scheme 1, pathway 1). However, we cannot specify where the addition site of •OH radicals is at this moment. Theoretically calculated FEDs have been recognized as a useful tool to predict initial attack site [14,15]. The addition of •OH radical usually take place at sites with higher $FED^2_{HOMO} + FED^2_{LUMO}$ value, while the direct photohole oxidation (i.e., electron extraction) can probably occur at the sites with higher values of $2FED^2_{HOMO}$ [14,15]. Thus, the FEDs data of lamivudine were calculated and summarized in Table 4. Higher $FED^2_{HOMO} + FED^2_{LUMO}$ values were obtained for C4 (0.5125), C5 (0.2843) and N3 (0.2953) indicating the initial •OH attacks were likely to occur on these three atoms. However, N3 site appeared to be unlikely due to stereo-hindrance effects. Thus, C4 and C5 was likely the initial addition site for •OH radicals.

On the other hand, the initial attack sites of hole, calculated from the values of $2FED^2_{HOMO}$, are likely to be N1 (0.2316), N3 (0.2814), C4 (0.8480), C5 (0.4172) and O13 (0.3325) atoms (Table 4). However, lamivudine should be firstly absorbed on the surface of TiO_2 at the beginning of the degradation because that the photoholes only can exist and attack the adsorption molecules within the surface of TiO_2 catalyst. As for lamivudine, the point charges were also calculated to explain the chemisorption pattern onto TiO_2 catalyst, and the data were also listed in Table 4. The relative more negative point charges were found at N1 (−0.705), N3 (−0.612) and O13 (−0.681), while more positive at C4 (0.189) and C5 (−0.488) atoms. Therefore, it was expected that N–CO–N fragment was the preferential site to be absorbed onto the surface of TiO_2 through the chemisorption model (Scheme S1), hence this functional group would be broken early in comparison with other atoms by direct photohole attack. Accordingly, the intermediates with m/z values of 136 and 112 were obtained from photohole attack at N3, labeled as intermediates (C) and (D), respectively. Then the intermediate (D) was further oxidized to (E) (with m/z value 129) by •OH radical and to (F) (with m/z value 69) by photohole attack with opening of aromatic ring (Scheme 1, pathway 2). In summary, the photohole oxidation and the addition of •OH radicals to the parent molecule are considered to be two main reaction pathways for lamivudine degradation.

To further elucidate the environment fate of lamivudine and its resulted degradation intermediates, the extent of mineralization was quantified by TOC concentration decrease and the evolution of inorganic ions during the photocatalytic degradation (Fig. 5). After 6 h irradiation, more than 83.0% of carbon contents in lamivudine was mineralized and completely converted into CO_2; 84.0% of sulphur atoms was released as SO_4^{2-} ions; and the nitrogen in lamivudine was also converted into different oxidation states (66.9% NH_3/NH_4^+ and 20.6% NO_3^- ions) by photocatalytic degradation. From all these results, it can be concluded that lamivudine

Table 4
Frontier electron densities and point charges on atoms of lamivudine calculated by using Gaussian 03 program at the B3LYP/6-31G* level.

Atom	$2FED^2_{HOMO}$	$FED^2_{HOMO} + FED^2_{LUMO}$	Point charge
N(1)	0.2316	0.2427	−0.705
C(2)	0.0012	0.0089	0.932
N(3)	0.2814	0.2953	−0.612
C(4)	0.8480	0.5125	0.189
C(5)	0.4172	0.2843	−0.488
C(6)	0.0042	0.2485	0.589
N(7)	0.0002	0.0813	−0.878
C(8)	0.0046	0.0135	0.327
O(9)	0.0024	0.0004	−0.623
C(10)	0.0006	0.0163	−0.116
S(11)	0.0168	0.0326	0.198
C(12)	0.0244	0.0792	−0.654
O(13)	0.3325	0.1721	−0.681
C(14)	0.0002	0.0034	−0.101
O(15)	0.0002	0.0002	−0.728

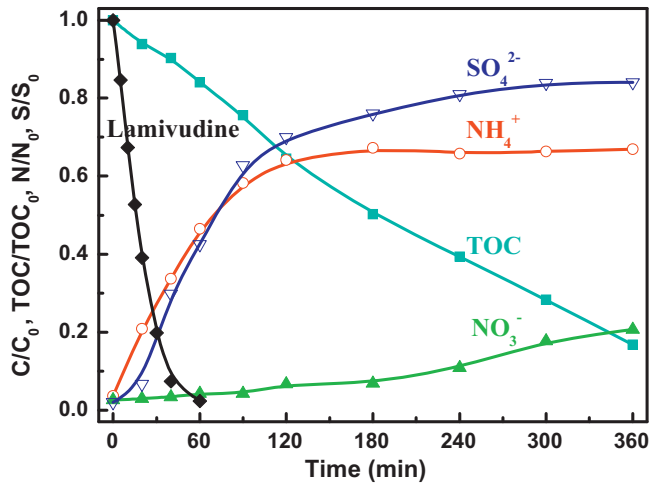

Fig. 5. Decrease of TOC and the evolution of sulphate, ammonium and nitrate ions during photocatalytic degradation of lamivudine: [Lamivudine] = 100 μM, [TiO_2] = 1.00 g L^{-1}, and pH value 7.0.

can be completely mineralized by the photohole oxidation and the hydroxyl radical attacks with enough degradation time, and the early degradation intermediates can be further converted into CO_2, H_2O and inorganic ions (NH_3/NH_4^+, NO_3^-, SO_4^{2-}) (Scheme 1).

4. Conclusions

The photocatalytic degradation kinetics was optimized by using both SVAT and CCD experiments. In addition, the photocatalytic degradation mechanism of lamivudine was also elucidated from HPLC/MS–MS results coupled with the calculated data of the FEDs and point charges. The remarkable conclusions can be summarized as follows:

1. Photocatalysis is an effective advanced oxidation technology for lamivudine decontamination. The degradation efficiencies depend on various affecting-parameters, such as TiO_2 concentration, pH value and initial lamivudine concentration. The SVAT optimal result indicated that lamivudine can be degraded efficiently within 60 min illumination at 1.00 g L^{-1} TiO_2 concentration, at pH value 9.0, and with initial lamivudine concentration of 100 μM.
2. Comparatively, the CCD based on RSM is a powerful tool to optimize and assess the individual and interaction effects of three independent variables on photocatalytic efficiencies. The conditions were optimized as TiO_2 concentration at 1.00 g L^{-1}, pH value at 6.7, and initial lamivudine concentration of 60 μM.
3. A tentative mechanism for photocatalytic degradation of lamivudine was proposed from both the experimental results of HPLC/MS/MS and the theoretical data of FEDs as well as point charges. The hydroxylation addition reaction (major) and the direct photohole oxidation (minor) are considered as two initial predominant pathways for photocatalytic degradation of lamivudine. The cleavage intermediates and the hydroxylation by-products may be mineralized completely into CO_2, H_2O and inorganic ions (NH_3/NH_4^+, NO_3^-, SO_4^{2-}) without generating any toxic final products during the photocatalytic degradation.

Acknowledgments

This is contribution no. IS-1393 from GIGCAS. The authors appreciate the financial supports from Knowledge Innovation Program of CAS (no. KZCX2-YW-QN103), NSFC (no. 40973068), and earmarked Fund of the SKLOG (SKLOG2009A02).

Appendix A. Supplementary data

Supplementary data associated with this article can be found, in the online version, at doi:10.1016/j.jhazmat.2011.09.077.

References

[1] J.D. Cahill, E.T. Furlong, M.R. Burkhardt, D. Kolpin, L.G. Anderson, Determination of pharmaceutical compounds in surface- and ground-water samples by solid-phase extraction and high-performance liquid chromatography–electrospray ionization mass spectrometry, J. Chromatogr. A 1041 (2004) 171–180.
[2] M. Clara, B. Strenn, N. Kreuzinger, Carbamazepine as a possible anthropogenic marker in the aquatic environment: investigations on the behaviour of Carbamazepine in wastewater treatment and during groundwater infiltration, Water Res. 38 (2004) 947–954.
[3] L. Guardabassi, D.M.A. Lo Fo Wong, A. Dalsgaard, The effects of tertiary wastewater treatment on the prevalence of antimicrobial resistant bacteria, Water Res. 36 (2002) 1955–1964.
[4] J.P. Sumpter, Xenoendocrine disrupters – environmental impacts, Toxicol. Lett. 102–103 (1998) 337–342.
[5] B. Halling-Sørensen, S. Nors Nielsen, P.F. Lanzky, F. Ingerslev, H.C. Holten Lützhøft, S.E. Jørgensen, Occurrence, fate and effects of pharmaceutical substances in the environment – a review, Chemosphere 36 (1998) 357–393.
[6] C. Prasse, M.P. Schlu¨sener, R. Schulz, T.A. Ternes, Antiviral drugs in wastewater and surface waters: a new pharmaceutical class of environmental relevance? Environ. Sci. Technol. 44 (2010) 1728–1735.
[7] G. Bedse, V. Kumar, S. Singh, Study of forced decomposition behavior of lamivudine using LC-MS/TOF and MS^n, J. Pharm. Biomed. Anal. 49 (2009) 55–63.
[8] L. Rizzo, S. Meric, M. Guida, D. Kassinos, V. Belgiorno, Heterogenous photocatalytic degradation kinetics and detoxification of an urban wastewater treatment plant effluent contaminated with pharmaceuticals, Water Res. 43 (2009) 4070–4078.
[9] T.C. An, H. Yang, W.H. Song, G.Y. Li, H.Y. Luo, W.J. Cooper, Mechanistic considerations for the advanced oxidation treatment of fluoroquinolone pharmaceutical compounds using TiO_2 heterogeneous catalysis, J. Phys. Chem. A 114 (2010) 2569–2575.
[10] H. Yang, G.Y. Li, T.C. An, Y.P. Gao, J.M. Fu, Photocatalytic degradation kinetics and mechanism of environmental pharmaceuticals in aqueous suspension of TiO_2: a case of sulfa drugs, Catal. Today 153 (2010) 200–207.
[11] V.A. Sakkas, P. Calza, C. Medana, A.E. Villioti, C. Baiocchi, E. Pelizzetti, T. Albanis, Heterogeneous photocatalytic degradation of the pharmaceutical agent salbutamol in aqueous titanium dioxide suspensions, Appl. Catal. B: Environ. 77 (2007) 135–144.
[12] S. Kaneco, N. Li, K.K. Itoh, H. Katsumata, K. Suzuki, K. Ohta, Titanium dioxide mediated solar photocatalytic degradation of thiram in aqueous solution: kinetics and mineralization, Chem. Eng. J. 148 (2009) 50–56.
[13] M. Pérez, F. Torrades, J. Peral, C. Lizama, C. Bravo, S. Casas, J. Freer, H.D. Mansilla, Multivariate approach to photocatalytic degradation of a cellulose bleaching effluent, Appl. Catal. B: Environ. 33 (2001) 89–96.
[14] X. Zhang, F. Wu, X.W. Wu, P.Y. Chen, N.S. Deng, Photodegradation of acetaminophen in TiO_2 suspended solution, J. Hazard. Mater. 157 (2008) 300–307.
[15] T.C. An, H. Yang, G.Y. Li, W.H. Song, W.J. Cooper, X.P. Nie, Kinetics and mechanism of advanced oxidation processes (AOPs) in degradation of ciprofloxacin in water, Appl. Catal. B: Environ. 94 (2010) 288–294.
[16] S. Horikoshi, H. Hidaka, Photodegradation mechanism of heterocyclic two-nitrogen containing compounds in aqueous TiO_2 dispersions by computer simulation, J. Photochem. Photobiol. A: Chem. 141 (2001) 201–207.
[17] H. Yang, T.C. An, G.Y. Li, W.H. Song, W.J. Cooper, H.Y. Luo, X.D. Guo, Photocatalytic degradation kinetics and mechanism of environmental pharmaceuticals in aqueous suspension of TiO_2: a case of beta-blockers, J. Hazard. Mater. 179 (2010) 834–839.
[18] D.F. Ollis, Kinetics of liquid phase photocatalyzed reactions: an illuminating approach, J. Phys. Chem. B 109 (2005) 2439–2444.
[19] A.V. Emeline, V.K. Ryabchuk, N. Serpone, Dogmas and misconceptions in heterogeneous photocatalysis. Some enlightened reflections, J. Phys. Chem. B 109 (2005) 18515–18521.
[20] T.C. An, Y. Xiong, G.Y. Li, C.H. Zha, X.H. Zhu, Synergetic effect in degradation of formic acid using a new photoelectrochemical reactor, J. Photochem. Photobiol. A: Chem. 152 (2002) 155–165.
[21] R.J. Candal, W.A. Zeltner, M.A. Anderson, Effects of pH and applied potential on photocurrent and oxidation rate of saline solutions of formic acid in a photoelectrocatalytic reactor, Environ. Sci. Technol. 34 (2000) 3443–3451.
[22] D.H. Kim, M.A. Anderson, Solution factors affecting the photocatalytic and photoelectrocatalytic degradation of formic acid using supported TiO_2 thin films, J. Photochem. Photobiol. A: Chem. 94 (1996) 221–229.
[23] M.R. Hoffmann, S.T. Martin, W. Choi, D.W. Bahnemann, Environmental applications of semiconductor photocatalysis, Chem. Rev. 95 (1995) 69–96.

[24] Y. Chen, S. Yang, K. Wang, L. Lou, Role of primary active species and TiO_2 surface characteristic in UV-illuminated photodegradation of Acid Orange 7, J. Photochem. Photobiol. A: Chem. 172 (2005) 47–54.
[25] C. Minero, G. Mariella, V. Maurino, D. Vione, E. Pelizzetti, Photocatalytic transformation of organic compounds in the presence of inorganic ions. 2. Competitive reactions of phenol and alcohols on a titanium dioxide–fluoride system, Langmuir 16 (2000) 8964–8972.
[26] A. Amine-Khodja, A. Boulkamh, C. Richard, Phototransformation of metobromuron in the presence of TiO_2, Appl. Catal. B: Environ. 59 (2005) 147–154.
[27] J. Rabani, K. Yamashita, K. Ushida, J. Stark, A. Kira, Fundamental reactions in illuminated titanium dioxide nanocrystallite layers studied by pulsed laser, J. Phys. Chem. B 102 (1998) 1689–1695.
[28] I.H. Cho, K.D. Zoh, Photocatalytic degradation of azo dye (Reactive Red 120) in TiO_2/UV system: optimization and modeling using a response surface methodology (RSM) based on the central composite design, Dyes Pigments 75 (2007) 533–543.
[29] J. Fernández, J. Kiwi, J. Baeza, J. Freer, C. Lizama, H.D. Mansilla, Orange II photocatalysis on immobilised TiO_2: effect of the pH and H_2O_2, Appl. Catal. B: Environ. 48 (2004) 205–211.
[30] J. Fernández, J. Kiwi, C. Lizama, J. Freer, J. Baeza, H.D. Mansilla, Factorial experimental design of Orange II photocatalytic discolouration, J. Photochem. Photobiol. A: Chem. 151 (2002) 213–219.